IEEE Access
Multidisciplinary | Rapid Review | Open Access Journal

Received October 22, 2019, accepted November 4, 2019, date of publication November 11, 2019,
date of current version November 20, 2019.

Digital Object Identifier 10.1109/ACCESS.2019.2952652

Protection Coordination Toward Optimal Network Reconfiguration and DG Sizing

MOHAMAD NORSHAHRANI ABDUL RAHIM[1,2], HAZLIE MOKHLIS[1], (Senior Member, IEEE), ABDUL HALIM ABU BAKAR[3], (Member, IEEE), MIR TOUFIKUR RAHMAN[4], OLA BADRAN[5], AND NURULAFIQAH NADZIRAH MANSOR[1]

[1]Department of Electrical Engineering, University of Malaya, Kuala Lumpur 50603, Malaysia
[2]Public Works Department, Menara Kerja Raya, Jalan Sultan Salahuddin, Kuala Lumpur 50580, Malaysia
[3]University Malaya Power Energy Dedicated Advance Center (UMPEDAC), University of Malaya, Kuala Lumpur 59990, Malaysia
[4]School of Engineering, RMIT University, Melbourne, VIC 3000, Australia
[5]Department of Electrical Engineering, Palestine Technical University – Kadoorie, Tulkarm 301, Palestine

Corresponding author: Hazlie Mokhlis (hazli@um.edu.my)

The authors would like to thank the University of Malaya for providing financial support under Research University (RU) Grants–Faculty Program (Grant No. GPF016A-2019).

ABSTRACT Research on network reconfiguration (NR) considering distributed generations (DG) is typically concerns on the issues of power loss, voltage deviation, DG sizing as well as its placement, which are important and required in the planning stage. On the other hand, another important aspect which often neglected in this stage is coordination of protection devices which is essential to prevent the network from damages following system breakdown. Without sufficient attention given to the protection coordination during NR, there is a possibility for the protective devices to miscoordinate and consequently lead to system blackout, due to changes in current flow and fault level. Therefore, this paper proposed an NR method for distribution networks with DG, incorporating protection devices. The proposed method aims to find the optimal configuration and DG size with minimum power loss, and at the same time ensuring protective devices operate correctly during normal and fault condition. Constraints on protection coordination and DG size are explicitly formulated in the proposed method. The validity of the proposed method is analyzed on three commonly used IEEE 33-bus, 69-bus and 118-bus distribution systems, employing the firefly algorithm (FA) and evolutionary programming (EP) algorithm. Comparative studies are done to prove the validity and robustness of the proposed method.

INDEX TERMS Network reconfiguration, protection coordination, distributed generations.

NOMENCLATURE

I_N	Branch current flow through the protective device
I_p	Protective device operating current
$I_f^{\min}$	Minimum fault current
I_{fault}	Fault current
$I_{pick-up}$	Pickup current
MCT	Maximum clearance time
MCT_{Fm}	Fuse maximum clearance time
MMT	Minimum melting time
MMT_{Fb}	Backup fuse minimum melting time
P_{loss}^R	Ratio of total active power loss
P_{loss}^{rec}	Total active power loss after NR
P_{loss}^0	Total active power loss before NR
P_{loss}	Total active power loss
$P_i^{\min}$	Minimum capacity of DG
$P_{DG,i}$	DG capacity at bus i
$P_i^{\max}$	Maximum capacity of DG
$P_{substation}$	Total power capacity generated from the substation.
$P_{load,n}$	Load at bus n
R_N	Resistance of branch N
t_{op}	Relay operating time
t_{fuse}	Fuse operating time
t_{fast}	Recloser operating time in fast-mode
PSM	Plug setting multiplier
TCC	Time current characteristic
TDS	Time delay settings

The associate editor coordinating the review of this manuscript and approving it for publication was Salvatore Favuzza.

CTI	Coordination time interval
DG	Distributed generation
DN	Distribution network
EP	Evolutionary programming
FA	Firefly algorithm
IDMT	Inverse definite minimum time
IEC	International Electrotechnical Commission
IEEE	Institute of Electrical and Electronic Engineering

I. INTRODUCTION

Continuous growth of electricity demand has made the power loss and voltage drop among dominant issues in distribution networks (DN), reducing the efficiency and reliability of the DN. In this regards, network reconfiguration (NR) could be employed as a relatively simple and low-cost approach to reduce power loss and improve the overall voltage profile. NR is defined as the process of changing the network's topology to achieve certain objectives by changing the state of the switches [1].

In the last decades, integration of distributed generation (DG), particularly in the form of renewable energy has increased tremendously as the sustainability and environmental issues come under scrutiny. From one perspective, DG integration further helps NR to reduce power loss and improve the voltage profile [2]–[6]. On the other hands, high DG integration also offers new challenges to the DN operators, especially from the perspective of protection systems reliability. Impacts brought by the DGs on the DN protection system must be carefully studied to ensure correct and timely operation of protection devices in times of need. In general, multiple connections of DG sources to DN alter the current flow and hence affect the coordination of protection devices.

Various protection strategies have been proposed to mitigate the impact of DG in DN using the conventional approach as well as modifications to the protection systems [7], [8]. But no strategies found for application during NR. A few works on NR with protection analysis did not take DG presence into considerations [9], [10]. For example, detail constraints on the NR method focusing on operation and coordination of fuse and relays as the protective devices are presented in [10] without considering the presence of DG. Integration of DG has been introduced in [11] to find optimal DG sizing and placement without changing the original protection systems. More advanced research has been presented in [12] where a protection and reconfiguration method was presented for DN with DG by network zoning. However, both analyses on NR in [11], [12] did not focus on power loss and voltage profiles issues. To the best of authors' knowledge, no studies have been done so far on the impact of protection coordination towards NR when DG is connected to minimize power loss and improve voltage profiles. Instead, researches on NR are more concerned only on the issues of power loss, voltage profile, DG sizing and location during planning stages [3], [13]–[18] while in the operational stage, the impact of protection system remains ignored.

In this study, the NR method is proposed with optimal DG connection considering protection coordination. The objective of this study is to obtain the optimal switching combination that provides minimum power loss and improved voltage profile, and simultaneously determine the optimal DG size, while the protective devices operate correctly for both normal and fault condition. Another key feature of the proposed work is that it utilizes the existing protection scheme without the needs for costly investment on new protection devices or alteration to the existing scheme. Modification to the existing protection system can potentially be a major obstacle towards the growth of DG penetration if it is not appropriately handled [11]. An optimization algorithm is systematically formulated in which the requirements imposed by the original protection system are treated as constraints in the optimization process. All the network constraints on reconfiguration and protection coordination are explicitly formulated and simultaneously considered to exclude the non-compliance switches combinations from the optimization process. The validity of the proposed algorithm is demonstrated through multiple case studies on the well-known IEEE 33-bus, 69-bus and 118-bus distribution test system. Metaheuristic techniques of Firefly Algorithm (FA) and Evolutionary Programming (EP) are employed in the proposed methodology. This paper, however, will not consider additions or changes to the existing protection devices in search of optimal network configuration, in line with the real-world practice of avoiding 'unnecessary' investment.

Main contributions of this paper are summarized as follows:

- Explicit consideration of protection devices coordination constraints in the NR process with DG connected. The proposed constraints prevent miscoordination of protection devices that might lead to network failure and equipment damages.
- Development of optimization process using FA and EP technique to simultaneously determine the optimal NR and the optimum DG sizing with consideration on protection coordination.
- Provide a good planning tool for the network operator to optimally size the DG in the network to reach better penetration level in compliance to existing system protection requirements.

The remaining of this paper is structured as follows: Section II discusses the impact of NR and DG on the protection system. In Section III, optimization solution with constraints of NR, protection system and DG sizing are formulated. Section IV presents the proposed protection strategy. Section V, VI and VII present and discuss the simulation results on the IEEE 33-bus, 69-bus and 118-bus system respectively. Analysis of consistency and computational time taken for the proposed method can be found in Section VIII. Finally, conclusions are presented in Section IX.

II. IMPACT OF NR AND DG ON PROTECTION SYSTEM

During the NR process, the line current change according to different switch combinations. If the new line current following NR exceeds the rating of the protective device, tripping will occur, cutting the power supply to the protected area. Violation of primary and backup protective device coordination is another consequence for not taking into account the constraints on the protection in parallel with NR. In addition, the protection of the new NR must be able to isolate the fault region from the fault current to avoid false tripping, fail to trip condition (blinding of protection) and miscoordination of protection devices. However, in practice, NR without changing the existing protection schemes is preferred by the network operator to avoid costly investments. Despite DG in DN help in significantly reducing power loss and improving voltage profile, protective devices might fail to accurately operate. This will subsequently cause unwanted power outage to the DN.

Numerous issues associated with the presence of DG in DN were discussed in [19], [20]. Among the issues are power quality problems, deterioration in the system efficiency, degradation in the system reliability, increase in short circuit level, coordination problems in relays, overvoltage and safety issues, sustained interruptions as well as voltage unbalance. From the protection perspective, the main issues caused by the connection of DG in DN can be categorized as (1) under fault condition and (2) under normal condition [21]–[23].

A. UNDER FAULT CONDITION

1) CHANGES IN FAULT LEVEL

Integration of DG to the DN increases the fault current level [21], [23]. Excessive fault levels might damage the system and trigger disruption to the power supply, in addition to cause injury to personnel. In that respect, changes in fault current should be monitored accordingly. The protection setting should be recalculated and reset following changes in the network topology. On the other hand, breaking capacity in the upstream feeder of typical DN is usually higher than the downstream feeder. However, with DGs integration, the fault current at the upstream might be lower than the breaking capacity of the protective devices which makes the protection system malfunctions.

2) PROTECTION MISCOORDINATION

In passive networks without DG, the fault current will typically flow from generation sources (upstream) towards fault location (downstream). In the presence of DGs, another source of fault current coming from the DG will flow to the fault location and cause miscoordination of protective devices. This will make the load feeder to sense an increment in the fault current while the upstream feeder senses a decrease in the fault current [21]. Continuously changing fault current may reduce the sensitivity of the protection system where for example, backup protection might operate before the primary and results in nuisance tripping to some of the loads affecting more areas.

3) BLINDING OF PROTECTION

Reverse power flow caused by DG integration would reduce the sensitivity of the line protection [21], [22]. Forward and reverse current which is smaller than the protection setting threshold value could 'blind' the protective devices and caused them to fail to operate.

4) SYMPATHETIC TRIPPING

Sympathetic tripping or unwanted tripping happens in the DN when one of the protection devices falsely trips or melted [21]. It differs from the nuisance tripping which is caused by the miscoordination issues.

5) ISLANDING

Islanding happens when parts of the DN is electrically isolated from the remainder of the main DN but remains to receive power from DG connected to the isolated subsystem. However, majority network operators prevent DG from operating in islanding mode [8].

B. UNDER NORMAL CONDITION

1) OVERVOLTAGE

Voltage profile in a distribution line can be influenced by the DG sources and frequent violation on the upper limit would stress the equipment involved [8].

2) POWER FLOW TO THE GRID

In a scenario where DG capacity is maximum during minimum load, excess power would flow reversibly from DN to the grid. Reverse power flow is usually prohibited to maintain the fault current and prevent other issues from DN to be transferred to the grid [13].

III. MATHEMATICAL FORMULATION AND CONSTRAINTS

A. OBJECTIVE FUNCTIONS

This study aims is to find the optimal NR with minimum power loss and voltage deviation, while ensuring existing protection devices remain coordinated and DG sizing is optimized.

The objective function, F of the optimization process can be described as follows [24]:

$$F = \min(P^R_{loss} + VD) \tag{1}$$

where P^R_{loss} is the ratio of total active power loss in the DN before and after the network reconfiguration as indicated by Eq. (2)

$$P^R_{loss} = \frac{P^{rec}_{loss}}{P^0_{loss}} \tag{2}$$

The total active power loss is a summation of losses in each line in the DN.

$$P_{loss} = \sum_{N=1}^{M} R_N \times |I_N|^2 \tag{3}$$

In Eq. (3), M is the number of a branch; R_N is the resistance of branch N; and I_N is the current flow through branch N.

Voltage deviation *(VD)* is the difference in measured voltage from the nominal value for each bus [24]. Smaller *VD* indicates better network condition.

$$VD = \max_{i=2}^{n} \frac{|V_1 - V_i|}{|V_1|} \quad i = 2, 3 \ldots n \tag{4}$$

where V_i in Eq. (4) is the measured voltage at bus i; n is the bus number in the DN; and V_1 is the nominal voltage.

Constraints considered in the optimization process can be divided into three groups; (i) network reconfiguration constraints; (ii) protection constraints and (iii) DG sizing constraints.

B. NETWORK RECONFIGURATION CONSTRAINTS

1) VOLTAGE MAGNITUDE

Inequality (5) would maintain the voltage of each bus within the allowable limit following the NR [14]. In this study, the limit is set at ±10% of the rated voltage.

$$V_{\min} \leq V_{bus} \leq V_{\max} \tag{5}$$

2) RADIAL CONFIGURATION

The network topology must be in radial after the reconfiguration process where the main substation must be connected to all the buses and there is no loop in the network. The function of graph theory in MATLAB is utilized to determine this radiality [14].

$$TF = graphisspantree(G) \tag{6}$$

$$TF = \begin{cases} 1 & radial \\ 0 & non-radial \end{cases} \tag{7}$$

where, G is the DN.

C. PROTECTION CONSTRAINTS

1) OVERLOAD FACTOR LIMIT

Under normal operating condition of the network, if the branch current is higher than the pick-up current of the relay or operating current of the fuse, the protective device must immediately isolate the coverage area to minimize damage to the distribution equipment. The overload factor (OLF) limit is formulated in Eq. (8) [25].

$$OLF \times I_N < I_p \tag{8}$$

Here, *OLF* is the overload factor, I_N is the branch current flow through the protective device after the reconfiguration; and I_p is the operating current of the protective device.

2) SENSITIVITY TO THE MINIMUM FAULT CURRENT

During fault, the optimal configuration must be ensured to provide higher current compared to the rating of the protective devices, I_p to avoid switches combinations that are not sensible to the minimum fault current, I_f^{min}. This will allow the protective device to sense the fault current and isolate the faulty region. This constraint will prevent protection blinding that left a certain portion of DN out of coverage and not protected [26].

$$I_p < I_f^{\min} \tag{9}$$

3) PROTECTION COORDINATION

When there are more than one protection devices connected in series, coordination among them under fault condition is required with multiple criteria. Determining the role of main and back-up for each protection devices is crucially important to avoid unnecessary tripping and undesired downtime to the DN. Moreover, the impact of DG on DN in terms of changes in fault current must be properly taken into account. In this study, three types of coordination are considered; fuse-fuse coordination, fuse-relay coordination and relay-recloser-fuse coordination.

a: FUSE-FUSE COORDINATION

In the protection coordination principle, the main fuse should operate first to isolate the fault before the back-up fuse operates. The criteria for the main fuse clearance time should not exceed 75% of the minimum melting time of back-up fuse [25].

$$MCT_{F_m} \leq 0.75 \times MMT_{F_b} \tag{10}$$

where MCT_{Fm} is maximum clearance time of the main fuse and MMT_{Fb} is the minimum melting time of the back-up fuse.

b: FUSE-RELAY COORDINATION

The coordination time interval (CTI) between the operation of downstream protective devices (as main protection) and relay as backup protection is considered in this study. This coordination ensures that the downstream protective device will operate to eliminate fault within the minimum time before the relay operates and guarantee the selectivity of the protection system as described by Eq. (11) [25].

$$t_{op} - t_{fuse} > CTI \tag{11}$$

In inequality (11), t_{op} is the relay operating time and t_{fuse} is the operating time of protective device at downstream.

Time delay setting (*TDS*) is the fine-tuning process to delay the relay operating time to achieve correct coordination. According to IEC 60255-151 standards [27], the operating time-current characteristic (TCC) of the relay is described by Eq. (12)

$$t_{op} = \frac{TDS \times \beta}{PSM^{\alpha} - 1} + L \tag{12}$$

where values for β, α and L are specified in the standards according to the different types of the selected relay operating

characteristics *PSM* is a plug setting multiplier, defined as the ratio of fault current and relay current setting or pick-up current according to Eq. (13).

$$PSM = \frac{I_{fault}}{I_{pick-up}} \tag{13}$$

c: RELAY-RECLOSER-FUSE COORDINATION

Value of recloser is set to change according to the specific network reconfiguration and this affects the relay-recloser-fuse coordination. The following constraint is applied for the programming to find the setting of recloser while at the same time, adhere to the recloser-fuse coordination constraint.

Prior to changing the reclosers setting, the effect on recloser-fuse coordination must be considered, especially in the coordination of the fast and slow operations of the recloser and fuses. When the fuse is at the load side and recloser is at the source side, the coordination criteria are specified below [10]:

a) The MMT (minimum melting time) of the fuse must be k times greater than the fast mode time of the recloser.

$$\frac{\text{MMT}}{t_{\text{fast}}} > k \tag{14}$$

b) The slow mode of the recloser must be greater than the MCT (max. clearance time) of the fuse. In other words, *CTI* between their operation times must be considered.

$$t_{relay} - -t_{device} > CTI \tag{15}$$

where t_{relay} is the relay operating time and t_{device} is the operating time of protective device at downstream. Similar to fuse-relay coordination, *CTI* is applied for coordination between recloser to relay.

D. DISTRIBUTED GENERATOR CONSTRAINTS

1) DISTRIBUTED GENERATOR CAPACITY

DG size at bus *i*, $P_{DG,i}$, is limited by the maximum and minimum capacity of the DG, $P_i^{\max}$ and $P_i^{\min}$, respectively [14].

$$P_i^{\min} \leq P_{DG,i} \leq P_i^{\max} \tag{16}$$

2) POWER INJECTION

Constraint to prevent power from DGs to flow to the grid and potentially disturb the grid protection system [26] is described by Eq. (17).

$$\sum_{i=1}^{k} P_{DG,i} < \sum_{n}^{nbus} (P_{load,n}) + P_{loss} \tag{17}$$

where k is the DG number; P_{load} is the load at bus n; *nbus* is the bus number; and P_{loss} is the overall active power losses in the DN.

3) POWER BALANCE

Eq. (18) ensures that the total power consumption by the load and power losses must be equal to the total power capacity generated from DGs and substation [14]. This is in line with the equilibrium principle which stated supply and demand of power must be equal.

$$\sum_{i=1}^{k} P_{DG,i} + P_{substation} = \sum_{n}^{nbus} (P_{load,n}) + P_{loss} \tag{18}$$

IV. PROPOSED STRATEGY

The proposed strategy aims to determine the optimal NR and optimal DGs output while ensuring protection constraints are satisfied. The strategy consists of two parts, executed simultaneously. Part 1 focuses on determining the optimal switching tie-bus to transform the network from its original form to the optimal reconfiguration, ensuring adherence to the formulation constraints. Simultaneously, task 2 computes the optimum DGs sizing at the specified location. In this work, it is assumed that the DG is privately-owned and its location is predetermined and agreed between the DG owners and network operator. Fig. 1 shows the flowchart of the proposed methodology, details of the steps will be discussed subsequently.

A. NR AND LOAD FLOW ANALYSIS

Load flow analysis is employed to compute the power loss, bus voltage and line currents and subsequently determine the value of the objective function. Radiality is ensured by opening the same number of switches as the number of normally open switch closed. Different combinations of switch statues are explored to find the minimum fitness function.

In this study, the initial five switches and the new five switches after the reconfiguration will be compared to find the optimal switching combinations.

The complexity of the NR process increased as the number of tie switches involved increased. DN with 5 tie switches, for example, would offer 435,897 different possibilities of configuration. It is thus prudent to apply an optimization technique to efficiently find the best configuration with the fittest objective function within this huge search space. For this reason, two meta-heuristic methods will be employed in this study as discussed in Section III.A, Objective Functions.

B. SIMULTANEOUS NR AND DG SIZING OPTIMIZATION USING FA AND EP

Firefly Algorithm (FA) and Evolutionary Programming (EP) algorithm have been successfully used to solve many power system problems [28]–[30]. For this reason, FA and EP were applied as the optimization technique to simultaneously optimize the NR and DG sizing. Ref. [31] and [18] details out the working principle of FA and EP respectively. The proposed algorithms are coded and executed in MATLAB platform.

C. PROTECTION SYSTEM

Constraints on protection as described in Section III.C are adopted in the optimization technique. Time-Current Characteristic (TCC) curves are used to analyse the impacts of NR and DG connection towards the performance, operation and coordination of the protection system, emphasizing the

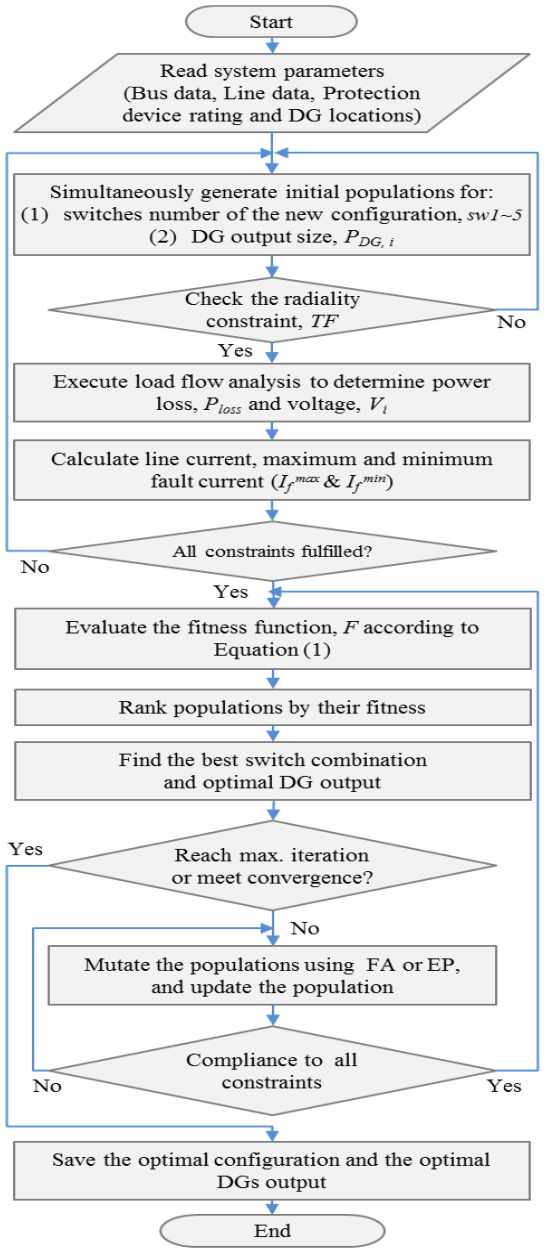

FIGURE 1. Flowchart of the proposed strategy to determine optimal NR with optimal DG size considering protection constraints.

compliance of the protection constraints for minimum and maximum fault current. Only configurations that satisfy all the specified criteria are considered for the evaluation of the objective function. The operating curves of the protective devices in this system are plotted in Fig. 3 based on their rating and the calculated minimum-maximum fault current values.

V. 33-BUS TEST SYSTEM

The validity of the proposed method is tested on three frequently used IEEE 33-bus [32], 69-bus and 118-bus systems. The one-line diagram of the 12.66kV, 33 bus system is shown in Fig. 2. The opened switches are represented as the dotted

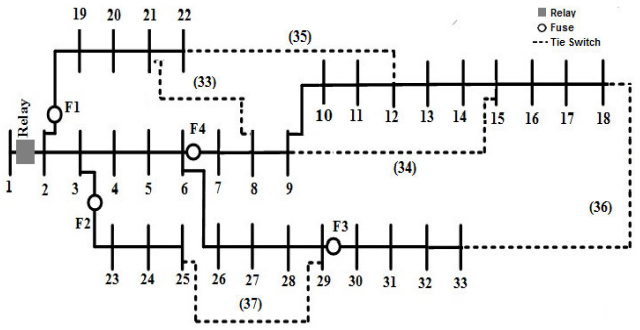

FIGURE 2. Initial 33-Bus test system with five tie switches and protective devices.

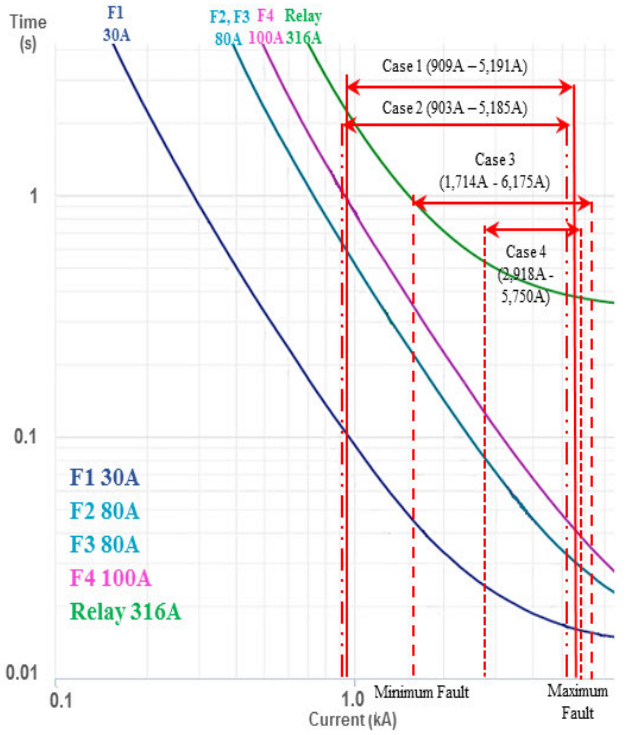

FIGURE 3. Log-log diagram of Time-Current Characteristic (TCC) operating curves generated based on relay, downstream fuses (MCT) and fault current.

TABLE 1. Data for initial configuration of the 33-bus network.

Parameter	Open switches	Active power loss (kW)	Minimum voltage (p.u.)
Value	33-34-35-36-37	202.7	0.9131

lines. The base apparent power is assumed to be 100MVA. Location and characteristics of the protective devices shown in Fig. 2 are according to [10]. A relay is installed at the main substation as the primary protection for the overall network, while four fuses are installed at the beginning of the laterals.

Table 1 presents the initial open switches combination, the existing total active power loss and the minimum voltage for the initial configuration.

DN can be categorized into two groups [33]; the first group is the fully automated distribution system which allows

changes on the protective device settings, while the second group is the partially automated network that employed a fixed size protective device such as a fuse. In this study, fuse is selected as a protective device for the proposed NR problem. Fuse is widely used in the existing DN especially in major rural overhead lines, due to its economic cost and proven performance. The main advantage of the fuse is its capability to safely interrupt huge short-circuit currents within its breaking capacity in a shorter time frame compared to a circuit breaker. Furthermore, fuse of a similar rating and breaking capacity is cheaper compared to the circuit breaker.

Fuse link type T is used in this study and its TCC is selected from products of S& C electric company [34]. In this study, CTI of 0.3 seconds is selected, while relay time dial is set to 0.15. IEC extremely inverse curve type was chosen for this Inverse Definite Minimum Time (IDMT) relay as it has an almost similar operating characteristic to the fuse TCC. Besides, these settings provide good coordination between fuse and relay.

Table 2 lists the rating of the protective devices and their coordination time during initial network configuration, as well as their load current.

TABLE 2. Protective device ratings and their coordination time in initial network configuration test system.

Protective Device	Current Setting (A)	Load Current (A)	Max. Short-Circuit Current (A)	*MCT* (s)	t_{op} (s)
Relay	316	209.6	5,943		
Fuse 1, F1	30	17.04	5,181	0.045	0.444
Fuse 2, F2	80	47.96	3,545	0.056	0.851
Fuse 3, F3	80	45.65	1,054	0.511	4.821
Fuse 4, F4	100	39.41	1,852	0.281	2.101

The operating curves of the protective devices are plotted in Fig. 3 based on their rating and calculated fault current values. The fuse curve represents the maximum clearance time (*MCT*).

For the maximum fault current, three phase to the ground bolted fault is assumed in the short-circuit calculations at the respective protective device location. While for the minimum fault current, the line to line fault is considered [35]. Note that the load current during fault condition is not taken into consideration in this study.

In this test system, four case studies as shown in Table 3 are performed to verify the operation and coordination of the protective system during NR. Case 1 and 2 are tested without DG integration, whereas Case 3 and 4 are tested with DG integration. To show the effectiveness of the protection strategy, Case 1 and 3 are simulated without protection constraints. In Case 2 and 4, the reconfiguration problem is solved with protective constraints.

A. CASE 1: OPTIMAL NR WITHOUT PROTECTION CONSTRAINTS

NR without protection constraints is performed in this case using FA and EP. The power loss and minimum voltage are

TABLE 3. Cases studies to verify the effectiveness of the proposed strategy.

Case Study	Scenario
Case 1	Optimal Network Reconfiguration (NR) without protection constraints (PC)
Case 2	Optimal NR considering PC
Case 3	Optimal NR with Optimum DG size and without PC
Case 4	Optimal NR with optimum DG sizing considering PC

TABLE 4. Comparing optimal configurations results between various optimization techniques.

Optimization techniques	Open switches	Power loss (kW)	Min voltage, (p.u.)
Proposed Firefly Algorithm (FA)	**7, 9, 14, 32, 37**	**139.5**	**0.9375**
Proposed Evolutionary Programming (EP)	7, 9, 14, 32, 37	139.5	0.9375
Selective Firefly Algorithm [36]	7, 9, 14, 32, 37	139.5	0.9375
Runner-Root Algorithm [37]	7, 9, 14, 32, 37	139.5	0.9375
Genetic algorithm [10]	7, 9, 14, 28, 32	139.9	0.9413
Particle swarm optimization [24]	7, 9, 14, 32, 37	139.5	0.9375
Fire work algorithm [16]	7, 9, 14, 28, 32	139.9	0.9413
Cuckoo search algorithm [24]	7, 9, 14, 32, 37	139.5	0.9375

tabulated in Table 4, along with values obtained by other meta-heuristic techniques from the literature. The opened switches for this optimal configuration are 7, 9, 14, 32 and 37. It can be observed that NR using FA and EP optimization technique reduced the power loss by 31.1% and improved the minimum voltage by 2.67%, compared to the initial configuration. It can also be concluded from the table that FA, EP and other techniques produce almost similar results and this confirms the validity of the proposed optimization technique. Hence the proposed techniques can be further tested by incorporating the protection constraints.

All fuse condition for the optimal configuration without protection constraints is further analyzed and the values are summarized in Table 5. Under the nominal condition, fuses F2, F3 and F4 operate accordingly under nominal loading and 25% overloading condition. However, fuse F1 is overloaded even under nominal loading condition where the load current passing through F1 will operate and meltdown the fuse link and break the circuit.

To prevent the impact of protection blinding, all four fuses will melt and break the circuits under fault condition as the minimum fault current is higher than the rating of the protective devices. The results show the importance of considering protection constraints during NR to prevent mal-operation of the protection system in the network.

In terms of coordination between the protection devices, the operation time of fuses and relay in the cases of minimum and maximum fault currents, as well as the operation curves plotted, are well-coordinated within the limits. TCC graph in Fig. 3 shows that each fuse has a different zone

TABLE 5. Protective devices condition in optimal configuration without protection constraints.

Protective device	Load current (A)	Load current with 25% overload (A)	Fault current (A)		Protective Device Condition
			Min.	Max.	
F1, 30A	**64.53**	**80.66**	**4,464**	5,191	**Open**
F2, 80A	47.76	59.70	**3,038**	3,533	Close
F3, 80A	41.18	51.47	**909**	1,057	Close
F4, 100A	7.25	9.06	**1,584**	1,842	Close

TABLE 6. Comparing optimal configurations results considering protection constraints between different optimization techniques.

Optimization technique	Open switches	Power loss (kW)	Min voltage, (p.u.)
Proposed FA	**11, 13, 32, 33, 37**	**181.1**	**0.9222**
Proposed EP	11, 13, 33, 36, 37	**181.9**	0.9192
Genetic algorithm [10]	10, 12, 32, 33, 37	**183.8**	0.9219

of protection. However, the obtained configuration is not feasible for NR since some fuses fail to operate properly in normal condition.

B. CASE 2: OPTIMAL NR CONSIDERING PROTECTION CONSTRAINTS

For Case 2, protection constraints are now considered during NR. Table 6 summarised the results where it can be seen that the power loss has increased compared to Case 1. However, this is expected as the considered protection constraints eliminate all switches combinations that violate the operation requirement of the protection system. Nevertheless, the increase in power loss is still lower than the active power loss observed prior to NR (initial case). The results support the needs to perform NR to improve network performance. Result also shows that the proposed method using FA and EP is performing better than the Genetic Algorithm [10] with 2.7kW and 1.9kW reduction in power loss respectively.

To verify the effectiveness of the proposed protection strategy, the operation and coordination of protective devices are analyzed. All fuses listed in Table 7 are found to be working properly in nominal loading and 25% overloading condition. The load current did not exceed the rating of the fuses under this case. TCC curves in Fig. 3 show that the relay and fuses coordination is satisfied. During fault condition, fuses will melt and trip the circuit due to minimum fault current.

C. CASE 3: OPTIMAL NR WITH OPTIMUM DG SIZING WITHOUT PROTECTION CONSTRAINTS

In this case, three DGs are assumed to be connected at Bus 31, 32, and 33 [15]. Sizing of each DG will be optimized to further reduce the total power loss and improve the voltage.

TABLE 7. Protective devices condition in optimal configuration considering protection constraints.

Protective device	Load current (A)	Load current with 25% overload (A)	Fault current (A)		Protective Device Condition
			Min.	Max.	
F1, 30A	23.34	29.17	4,459	5,185	Close
F2, 80A	47.93	59.91	3,041	3,536	Close
F3, 80A	41.87	52.34	903.0	1,050	Close
F4, 100A	36.85	46.06	1,590	1,849	Close

TABLE 8. Comparing optimal configurations results without considering protection constraints with optimum DG sizes connected.

Technique	Open switches	Power loss (kW)	Losses reduction (%)	Min. voltage (p.u.)	DG Output, (MW)	Objective Function, F
Proposed FA	**7, 10, 13, 28, 32**	**72.36**	64.30	**0.9751**	DG1:0.676 DG2:0.516 DG3:0.633 Total:1.825	**0.4103**
Proposed EP	7, 10, 27, 32, 34	73.34	63.84	0.9732	DG1:0.615 DG2:0.575 DG3:0.595 Total:1.785	0.4171
HSA [6]	7, 10, 14, 28, 32	73.05	63.95	0.9700	DG1:0.5258 DG2:0.5586 DG3:0.5840 Total: 1.6684	0.4186
EP [13]	7, 8, 9, 28, 32	73.97	63.51	0.9710	DG1:0.7024 DG2:0.6390 DG3:0.6224 Total: 1.964	0.4223

The minimum and maximum capacity of the DG is set to be 0.5 MW and 1.5 MW, respectively. The maximum DG penetration is limited to 3.5 MW, which is a practical constraint as compared to the overall load of 3.7 MW in the network. In this study, DG is assumed to inject only active power and is of a synchronous machine type as the electronically-interfaced DGs has limited fault current which may not be exposed to protection coordination issues.

From the simulation result in Table 8, by optimizing the DG sizes, power loss is reduced significantly to 72.36 kW compared to Case 1 (139.5 kW) and Case 2 (181.1 kW). It shows that by adopting DG into the network will further reduce the power loss. Table 8 also points out the configurations and results for a similar case found in [6] and [13] where the proposed methods produce slightly better results in terms of the objective function and thus confirm the validity of the proposed optimization technique.

Although DG has further reduced the power loss, protection devices are found to be overloaded. Optimization results tabulated in Table 9 shows that Fuse 1 is overloaded even under nominal condition though other protective devices operate normally under nominal and 25% overloading condition. Hence, this configuration is not feasible for practical implementation as it affects the operation of the protection system. Coordination between relay and fuses are correct, but fuse F2 and F3 are not coordinated accordingly as can

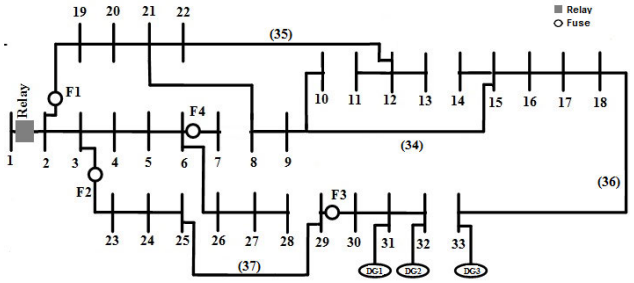

FIGURE 4. Optimal configuration connected with optimum DG sizing without protective constraints for 33-bus (Case 3).

TABLE 9. Protective devices condition in optimal configuration connected to DGs without protection constraints.

Protective device	Load current, A	Load current with 25% overload, A	Fault current, A		Protective Device Condition
			Min.	Max.	
F1, 30A	**42.25**	**52.82**	5,311	6,175	**Open**
F2, 80A	51.21	64.01	4,267	4,962	Normal
F3, 80A	9.60	12.00	5,094	5,923	Normal
F4, 100A	7.12	8.89	1,714	1,993	Normal

be seen in Fig. 4. In the case of network fault, the network will experience unwanted tripping in which both main fuse F3 and backup fuse F2 with the same rating (80A each) will trip simultaneously since there is insufficient current and time discrimination between them.

From Table 9, it can also be observed that the short circuit currents in network connected with DG increased extensively compared with Case 1, where the increment range from 0.1 kA to 4.8 kA, depending on the network configuration, fault and DG location. The highest increment was at fuse F3 as it is located closer to DGs locations. Nevertheless, TCC curves in Fig. 3 confirm that the coordination between all protective devices still exists within the fault current range.

D. CASE 4: OPTIMAL NR WITH OPTIMUM DG SIZING CONSIDERING PROTECTION CONSTRAINTS

Extension of Case 3 is performed under Case 4 where constraints on the protection system are considered. Additionally, DGs are connected to bus 14, 24 and 30 to compare effects of DG location to the overall objective function. From the results presented in Table 10, in terms of the objective function, an optimal network configuration with DG located at the lateral ends (i.e. bus 31, 32, 33 as shown in Fig.5) is performing better than the optimal configuration when DG location is diversified. Even though power loss in both Case 4 higher than the losses obtained in Case 3, it can still be concluded that optimization considering protection constraints is better as it produced feasible solutions for real-life implementation.

Table 11 shows that protection constraints are fulfilled under normal load condition and 25% overloading condition. The minimum fault current is higher than the protective device and thus will be able to melt the fuse and isolate

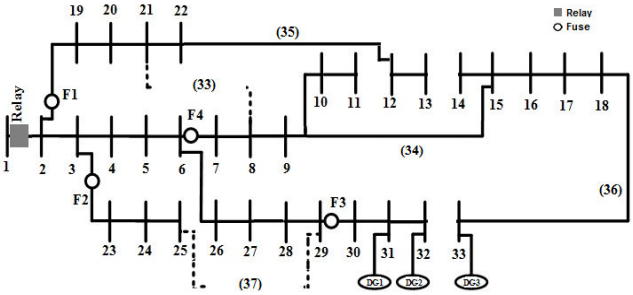

FIGURE 5. Optimal network configuration connected with optimum DG sizing considering protection constraints for 33-bus (Case 4).

TABLE 10. Comparing optimal configurations results considering protection constraints with optimum DG sizes at different locations using FA and EP for 33-bus (Case 4).

Technique,	DG Location	Open switch	Power loss, kW	Losses reduction (%)	Min. voltage p.u.	DG Output, MW	Obj. Func. F
Proposed FA	31, 32, 33	**11, 13, 32, 33, 37**	**91.02**	55.10	**0.9720**	DG1:0.6654 DG2:0.5949 DG3:0.6055 Total:1.866	**0.5055**
Proposed EP	31, 32, 33	11, 31, 33, 34, 37	93.30	53.97	0.9626	DG1:0.514 DG2:0.537 DG3:0.520 Total: 1.571	0.5259
Proposed EP	14, 24, 30	11, 13, 15, 33, 37	91.99	54.62	0.9394	DG1:0.525 DG2:0.602 DG3:0.603 Total: 1.73	0.5419

TABLE 11. Protective devices condition in optimal configuration connected to DGs considering protection constraints.

Protective device	Load current, A	Load current with 25% overload, A	Fault current, A		Protective Device Condition
			Min.	Max.	
F1, 30A	23.31	29.13	4,945	5,750	Normal
F2, 80A	47.57	59.46	3,553	4,131	Normal
F3, 80A	12.38	15.47	4,168	4,846	Normal
F4, 100A	27.35	34.18	2,918	3,393	Normal

the affected area in the network when fault happened. DG penetration has increased the fault current level in the area covered by the respective protective device. The highest fault current is 5.75 kA when three phase fault occurs. With DG in the network, the fault impedance decreased due to parallel circuits resulting in the increased fault level. Depending on the equipment damage curve, this puts certain distribution equipment at risk as they might not be designed to operate under these circumstances. However, the proposed work in optimizing the DG sizing has helped in limiting the total fault current. This in turns helps to avoid damage to the equipment and prevents the consequent risk of injury to personnel and interruption to power supplies.

From Fig. 6, although DGs connection increase the maximum fault current seen by the protective devices, the TCC curves show that coordination between relay as main protection and downstream fuses as backup protection system is held within the range of minimum and maximum

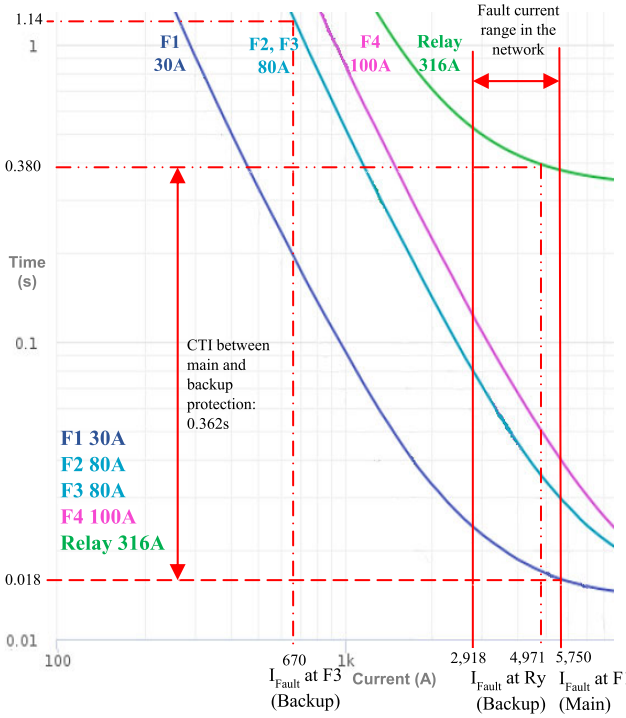

FIGURE 6. Minimum-maximum fault current region and sympathetic tripping impact analysis for fault at F1 due to multiple source directions.

fault currents. At the maximum fault current condition for fault at the line connecting bus 2 and 19, operating time of fuse F1 as the main protection takes 0.018 seconds to melt. If it fails to clear the fault, relay and fuse F3 as backup protection will operate in 0.380 seconds and 1.14 seconds respectively to clear the fault. The difference in this operating time or also known as CTI is 0.362 seconds which has satisfied the protection constraint that requires more than 0.3 seconds. CTI between main and backup protection cannot be too long as late backup action will cause damage to the equipment. Sufficient coordination will allow the protection devices to clear the short circuit within the time limit to ensure the thermal stresses can be withstood by the protected cable and other distribution equipment.

In a case when a fault happens at the end of the radial line, for example in a line connecting bus 18 and 33, DG3 will form an island and will be disconnected from the network as required by IEEE 1547 Standard [38]. Each DG is assumed to have its own interconnect protection at point of common coupling (PCC) to avoid continuous fault current to the network. The interconnect protection provides the protection scheme on the DN-side for parallel operation of the DG and the DN. This requirement is normally established by the network operator. The protection device setting value for this interconnects protection can be referred to the proposed optimal DGs size of 665 kW (DG1), 594 kW (DG2) and 605 kW (DG3). These DGs size comply with the constraints as in Eq. (17). The optimal DG size has mitigated issues of reverse power flow from DG to the grid as described by Eq. (18).

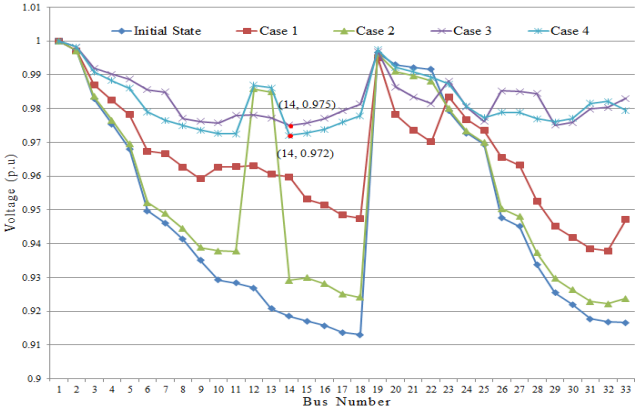

FIGURE 7. Voltage profile of IEEE 33-bus network for initial configuration and different cases.

TABLE 12. Analysis of sympathetic tripping effect for different fault locations due to multiple sources directions.

Fault location		Source of Fault Current Directions			Minimum *CTI* (s)	Sympathetic tripping?
		Grid	DG1 and DG2	DG3		
F1	Protective device affected	F1 melt	F3 did not melt due to lower I_{fault}	F4 did not melt due to lower I_{fault}		**No**
	I_{fault} (A)	5,750	670	327		
	Operating time (s)	0.018	1.14	5.63	**1.12**	
F2	Protective device affected	F2 melt and Fault isolated	F3 did not melt due to lower I_{fault}	F4 did not melt due to lower I_{fault}		**No**
	I_{fault} (A)	4,131	626.2	303.2		
	Op.time (s)	0.042	1.47	18.5	1.43	
F3	Protective device affected	F3 melt	DGs inter-connection protection activated	F4 did not melt due to lower I_{fault}		**No**
	I_{fault} (A)	4,846	1,601	266.7		
	Op.time (s)	0.037	Instantaneous trip	256	255.9	
F4	Protective device affected	F4 melt	F3 did not melt due to lower I_{fault}	DGs inter-connection protection activated		**No**
	I_{fault} (A)	3,393	1,017	705.8		
	Op.time (s)	0.093	0.57	Instantaneous trip	0.48	

In addition, it helps to optimize the capital investment cost to build the DG facility.

Impact of sympathetic tripping is also avoided using the proposed approach. Referring to Fig. 5 and 6, when a fault happens at F1, high fault current from DG1 and DG2 may lead to false operation of fuse F3, particularly when the capacity of DG is big. However, since the DG size is optimized in this case, the false operation is prevented. Sufficient CTI will allow fuse F1 as main protection to isolate the faulty area before other protective devices operate as a backup. Fault current flowing to the fault location comes from different

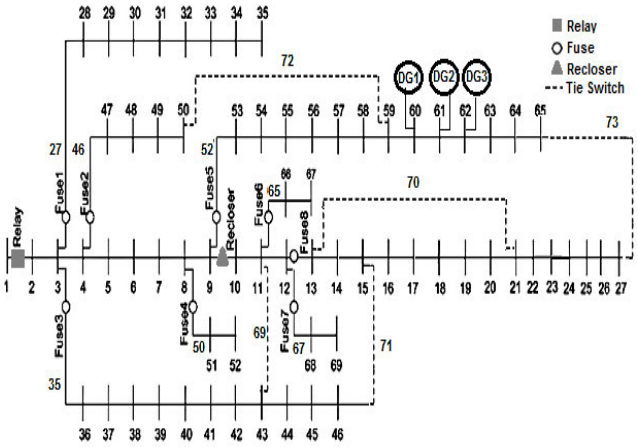

FIGURE 8. Initial 69-Bus test system with five tie switches, protective devices and DGs.

TABLE 13. Comparing initial configuration and optimal configuration results for Case 5 and Case 6 with optimum DG size connected (69 bus).

Technique	Open switches	Power loss (kW)	Min. voltage (p.u.)	DG Output, (MW)	Objective Function, F
Initial Condition					
	69, 70, 71, 72, 73	224.56	0.9093	Without DG	1.1172
Case 5 (without protection constraints)					
Proposed FA	**12, 57, 61, 69, 70**	**39.54**	**0.9816**	DG1:0.260 DG2:1.228 DG3:0.447 Total:1.935	**0.2230**
Proposed EP	12, 19, 57, 61, 69	40.34	0.9816	DG1:0.251 DG2:1.232 DG3:0.452 Total:1.935	0.2266
HSA [6]	13, 17, 58, 61, 69	40.30	0.9736	DG1:0.3525 DG2:1.0666 DG3:0.4527 Total:1.871	0.2342
Case 6 (considering protection constraints)					
Proposed FA	**13, 18, 42, 49, 70**	**126.8**	**0.9500**	DG1: 0.502 DG2: 0.591 DG3: 0.826 Total: 1.919	**0.6424**
Proposed EP	14, 41, 48, 64, 70	150.4	0.9640	DG1: 0.664 DG2: 1.209 DG3: 0.849 Total: 2.722	0.7339

sources direction i.e. Grid (Bus 1), DG1, DG2 and DG3. In this scenario, the interconnect protection of all DGs will act as backup protection to fuse F3 and F4 if both fail to operate. If the failure of fuse F3 and F4 happen, relay at each DGs will sense current flow higher than the normal rating and hence trip instantaneously in 0.1 seconds. As shown in Table 12, CTI for the worst case is more than 0.3 seconds. This proves that coordination between main and backup protective devices for the proposed optimal configuration has remained effective without sympathetic tripping impact. Similar results are found for different fault location at F2, F3 and F4 as presented in Table 12.

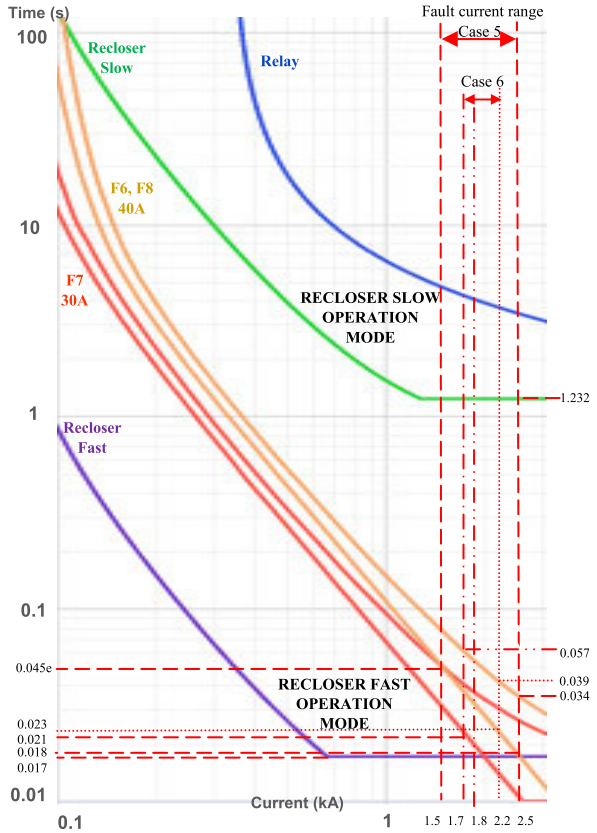

FIGURE 9. TCC coordination between recloser and downstream fuses (F6, F7, F8) in fast and slow mode operation generated based on Case 5 and 6 for 69-bus test system.

TABLE 14. Protective devices condition in optimal configuration connected to DGs without protection constraints.

Protective device	Load current (A)	Load current with 25% overload (A)	Fault current (A)		Protective Device Condition
			Min.	Max.	
Relay, 336A	161.28	185.47	6,879	7,999	Close
F1, 10A	4.71	5.41	6,789	7,895	Close
F2, 80A	**86.71**	**99.72**	6,818	7,928	**Open**
F3, 20A	**35.40**	**40.71**	6,802	7,909	**Open**
F4, 6A	2.66	3.06	3,453	4,016	Close
F5, 200A	3.33	3.83	3,213	3,736	Close
Recloser, 67A	24.07	27.69	2,469	2,871	Close
F6, 40A	2.10	2.41	2,147	2,496	Close
F7, 30A	3.29	3.78	1,494	1,738	Close
F8, 40A	0.00	0.00	1,315	1,529	Close

TABLE 15. Coordination between recloser and downstream fuses in fast and slow mode operation without protection constraints.

Device	Fault Current (A)		Fast Operation Mode			Slow Operation Mode		
	Min.	Max	t_{op} (s)	*MMT* (s)	Coordination factor, *k*	t_{op} (s)	*MCT* (s)	*CTI*: t_{op}- *MCT* (s)
F6	2,147	2,496	0.017	0.018	**1.06**	1.232	0.034	1.198
F7	1,494	1,738	0.017	0.021	**1.24**	1.232	0.039	1.193
F8	1,315	1,529	0.017	0.045	2.65	1.232	0.072	1.16

E. VOLTAGE PROFILE ANALYSIS

As presented in Case 4, the proposed method considering protection constraints and optimal DG sizing has significantly

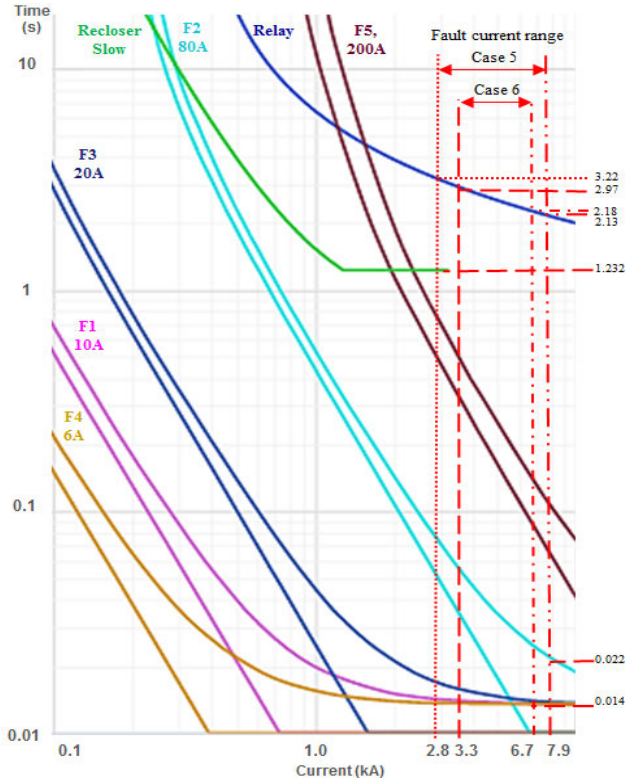

FIGURE 10. TCC coordination between relay and downstream protective devices (recloser, fuses F1 to F5) generated based on Case 5 and 6 for 69-bus test system.

TABLE 16. Coordination between relay and downstream devices without considering protection constraints.

Downstream device and its fault location	Max. fault current at device location (A)	t_{op} (s)	Downstream device operating time, (s)	*CTI* (s)
Recloser	2,871	3.22	1.232	1.988
F2	7,928	2.131	0.022	2.109

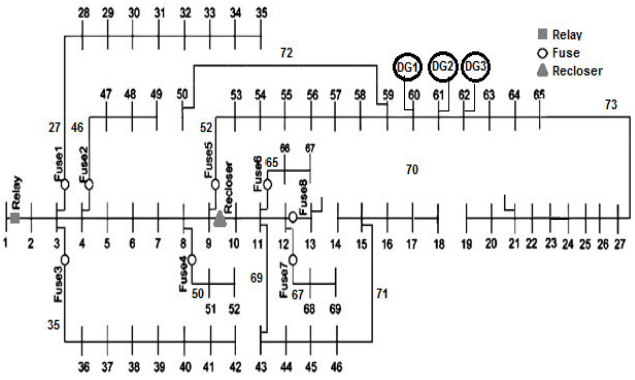

FIGURE 11. Optimal network configuration connected with optimum DG sizing considering protection constraints for 69-bus (Case 6).

improved the minimum bus voltage compared to the initial case. The lowest voltage found by the proposed method after NR is 0.9720 p.u. at bus 14. The voltage magnitude

TABLE 17. Protective devices condition in optimal configuration considering protection constraints with DGs connected.

Protective device	Load current (A)	Load current with 25% overload (A)	Fault current, (A)		Protective Device Condition
			Min.	Max.	
Relay 336A	164.17	188.79	5,8449	6,796	Close
F1, 10A	4.70	5.41	5,7788	6,720	Close
F2, 80A	23.90	27.49	5,7779	6,719	Close
F3, 20A	5.20	5.98	5,7788	6,720	Close
F4, 6A	2.68	3.08	4,1902	4,872	Close
F5, 200A	57.47	66.09	4,2418	4,932	Close
Recloser 67A	39.83	45.81	2,8537	3,318	Close
F6, 40A	2.12	2.44	2,0236	2,353	Close
F7, 30A	3.33	3.83	1,6142	1,877	Close
F8, 40A	0.46	0.53	1,4957	1,739	Close

TABLE 18. Coordination between recloser and downstream fuses in fast and slow mode operation considering protection constraints.

Device	Fault Current (A)		Fast Operation Mode			Slow Operation Mode		
	Min.	Max	t_{op} (s)	*MMT* (s)	Coordination factor, *k*	t_{op} (s)	*MCT* (s)	*CTI*: (t_{op}- *MCT*) (s)
F6,40A	1,885	2,192	0.017	0.023	1.35	1.232	0.039	1.193
F7,30A	1,442	1,677	0.017	0.024	1.41	1.232	0.041	1.191
F8,40A	1,496	1,739	0.017	0.035	2.06	1.232	0.057	1.175

TABLE 19. Coordination between relay and downstream devices considering protection constraints.

Downstream device and its fault location	Max. fault current at device location (A)	Protection device operating time, (s)		
		Upstream	Downstream	*CTI*
Recloser	3,318	2.975	1.232	1.743
Fuse, F1	6,720	2.185	0.014	2.171

for each bus in all cases is plotted in Fig. 7. It shows that the inclusion of DG in Case 3 and Case 4 has resulted in a beneficial bus voltage improvement. As a whole, the voltage at each bus following NR for all cases was well kept within the allowable minimum limit of 0.9 p.u. Although Case 3 provides a better minimum voltage magnitude of 0.9751 p.u. at bus 14, the obtained optimal configuration violated the protection constraints. This would result in certain fuses melted down and blackout happens in a certain area.

VI. 69-BUS TEST SYSTEM

In order to show the robustness of the proposed method, two case studies were performed on a medium distribution network of IEEE 69-bus test system in the presence of DGs under different cases; Case 5 without protection constrains and Case 6 considering protection constraints. IEEE 69-bus consists of 69 buses, 68 lines and 5 tie switches. Other network parameters can be found in [39]. DGs are assumed to be connected at bus 60, 61, and 62 based on [6]. Details for the initial configuration are shown in Table 13 and the one-line

TABLE 20. Comparing initial configuration and optimal configuration results for Case 7 and 8 with optimum DG size connected (118 bus).

Technique	Open switches	Power loss (kW)	Min. voltage (p.u.)	Obj. Function, F	DG Output, DG 1-3 (MW)
Initial Condition					
	118 to 132	1,298.0	0.8688	1.1565	Without DG
Case 7 (without protection constraints)					
Proposed FA	**22, 25, 33, 39, 42, 58, 70, 82, 86, 97, 117, 121, 122, 125, 130**	**591.72**	**0.9632**	**0.4927**	2.602, 3.525, 3.174 Total: 9.301
Proposed EP	22, 26, 33, 43, 60, 70, 82, 97, 121, 122, 124, 125, 127, 130, 131	607.56	0.9574	0.5107	3.112, 2.966, 3.374 Total:9.452
ACSA [41]	42, 25, 22, 121, 122, 58, 39, 125, 70, 127, 128, 81, 130, 131, 33	597.95	0.965	0.4953	2.533, 3.704, 3.682 Total:9.919
Case 8 (considering protection constraints)					
Proposed FA	**24, 45, 59, 74, 98, 120, 121, 122, 124, 125, 126, 129, 130, 131, 132**	**659.17**	**0.9528**	**0.5550**	2.9133, 2.5251, 2.8741 Total: 8.313
Proposed EP	26, 42, 58, 74, 75, 120, 121, 123, 124, 125, 126, 129, 130, 131, 132	712.29	0.9382	0.6106	2.7015, 2.3611, 1.828 Total: 6.891

diagram of the 69-bus system is shown in Fig. 8. Table 13 also shows the results of optimal NR for Case 5 and Case 6.

The position, size and type of protective devices were considered following Ref. [10], based on the initial configuration of the network. Note that 69-bus system has an extra protective device i.e. recloser, located at the outgoing feeder of bus 9. It was used to segregate the protection zone of the main network branch. Hence, analysis on this 69-bus system will consist of coordination between; (1) recloser and downstream fuses and, (2) relay with downstream devices.

Recloser has two modes of operation; a fast mode that trips the circuit for temporary fault before the downstream fuse operates, and a slow mode that functions as backup protection once the downstream fuse fails to operate. In the case where both fuses and recloser fail to isolate the fault, the relay will become the next backup protection. The fault current must be kept within the specified minimum and maximum limits for this sequential operation to happen as shown in Fig. 9 and 10.

Correct coordination must be ensured between recloser and fuses F6, F7 and F8 as shown in network diagram of Fig. 8. In this case, the recloser is assumed to have one fast and one delayed operation only. The time-dial setting (TDS) for the relay is set at 1.5, while TDS for recloser in fast mode is 0.05 and the slow mode is 1.0. Eq. (11) specified that the coordination factor, k for the recloser in fast mode to be 1.25. *CTI* considered for the coordination of recloser in slow mode with fuses, and the coordination of relay with its downstream devices in this network is 0.2 seconds.

TABLE 21. Protective devices condition in optimal configuration connected to DGs without protection constraints.

Protective device with rating/setting.	Load current (A)	Load current with 25% overload (A)	Fault current (A)		Protective Device Condition
			Min.	Max.	
Relay 1, 900A	464.34	580.43	13,063	15,189	Close
Relay 2, 562A	290.73	363.41	11,391	13,245	Close
Relay 3, 433A	169.84	212.30	10,488	12,196	Close
Recloser 1, 120A	52.48	65.60	5,766	6,705	Close
Recloser 2, 530A	208.92	261.14	8,061	9,373	Close
Recloser 3, 250A	55.36	69.20	6,683	7,771	Close
Recloser 4, 375A	187.14	233.93	7,787	9,055	Close
Recloser 5, 200A	111.88	139.86	4,797	5,578	Close
F1, 50A	31.15	38.94	5,750	6,686	Close
F2, 40A	0.00	0.00	5,399	6,278	Close
F3, 30A	**179.00**	**223.75**	8,468	9,847	**Open**
F4, 140A	8.80	11.00	8,061	9,373	Close
F5, 20A	4.39	5.49	1,276	1,483	Close
F6, 80A	33.47	41.84	7,844	9,121	Close
F7, 80A	**65.14**	**81.42**	5,621	6,536	**Open**
F8, 200A	9.43	11.79	5,984	6,958	Close
F9, 140A	39.05	48.81	5,703	6,631	Close
F10, 100A	54.88	68.60	3,905	4,540	Close
F11, 30A	15.55	19.44	3,870	4,500	Close
F12, 140A	37.35	46.69	6,279	7,301	Close
F13, 40A	**58.10**	**72.62**	7,359	8,557	**Open**
F14, 140A	59.25	74.06	3,304	3,842	Close
F15, 65A	21.04	26.30	3,253	3,783	Close
F16, 140A	88.43	110.53	4,511	5,245	Close
F17, 50A	26.79	33.49	6,201	7,,211	Close

A. CASE 5: OPTIMAL NR WITH OPTIMUM DG SIZING WITHOUT PROTECTION CONSTRAINTS

The optimal network configuration for Case 5 is shown in Table 13. From the aspect of protection system compliance, Table 14 shows that all fuses perform correctly in both normal and overload situation, except fuse F2 is overloaded in both normal and 25% overload condition. Each minimum fault current values are high enough to melt the respective fuses in their protective region during fault condition, thus prevent the effect of protection blinding. TCC curves on coordination for recloser with downstream fuses, and relay with its downstream devices are plotted in Fig. 9 and 10, respectively.

Table 15 summarizes the coordination of operating time for recloser in fast and slow operation mode. It can be seen that the coordination factor for all fuses is higher than 1.25 as required by Eq. (11). Hence, the coordination in fast mode is held. However, coordination of slow mode is not satisfied when fault happens at F6 where CTI is 0.193 seconds, lesser than the 0.2 seconds requirement. These facts are confirmed through Fig. 9, where the coordination between recloser and fuses in the fast mode is held in the fault current range of the protection region. While for the slow mode, coordination failed to meet the CTI requirement.

Table 16 shows operating time for relay and its downstream devices, along with CTI between their operations. The operating curves of relay and its downstream devices are presented in Fig. 10. According to Table 16 and Fig. 10, CTI for recloser and fuse fulfil the 0.2 seconds requirement which proves the correct coordination is reached.

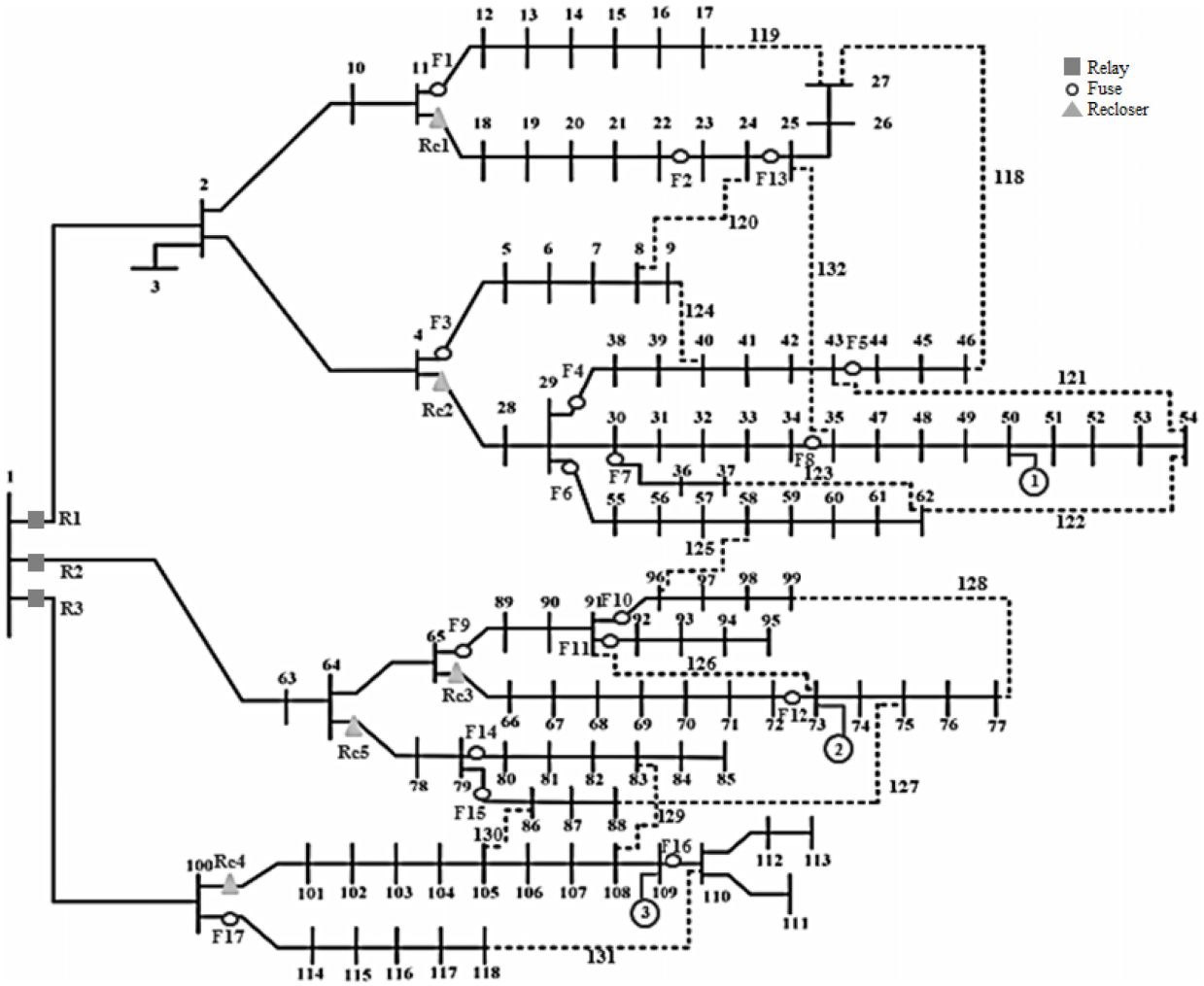

FIGURE 12. Initial 118-Bus test system with 15 tie switches, relays, reclosers, fuses, and DGs.

B. CASE 6: OPTIMAL NR WITH OPTIMUM DG SIZING CONSIDERING PROTECTION CONSTRAINTS

The optimal network configuration for this case is shown in Fig. 11 by referring to results in Table 13. It can be seen from the table that the proposed method performs better than the initial configuration in terms of power loss reduction and voltage profile improvement. Nevertheless, power loss increases by 87.26 kW compared to Case 5 which does not consider protection constraints.

Load current passing through each protective device is tabulated in Table 17. All devices operate accordingly during normal and overload condition and able to detect minimum fault current in the protection region.

Table 18 shows that the recloser fast mode operation has fulfilled the constraint for coordination factor, k to be more than 1.25. This indicates that the fast mode operating time of the recloser is 25% faster than the minimum melting time of the fuses. Therefore, coordination in fast mode is held. For slow mode operation, it can be observed that coordination between recloser and downstream devices has fulfilled the protection constraint requirement, where all CTIs are more than the 0.2 seconds. From Fig. 9, it can be concluded that the coordination of the recloser with downstream fuses for this case is held.

In Table 19, relay and downstream devices coordination were held with CTI more than 0.2 seconds. Fig. 10 indicates that coordination of the relay with recloser, and relay with downstream fuses is held.

VII. 118-BUS TEST SYSTEM

This large DN test system consists of 3 feeders, 118 buses, 117 lines and 15 tie switches. The complete bus and line data can be found in [40]. Three DGs are connected at bus 50, 73 and 109, respectively, based on optimal location found by [41]. The type, size and location of the protective devices are assumed to follow the concept proposed in [10] in the

TABLE 22. Coordination between reclosers and downstream fuses in fast and slow mode operation without protection constraints.

Protection Device		Fault Current at Downstream (kA)		Fast Operation Mode			Slow Operation Mode		
Up stream	Down stream	Min.	Max	t_{op} (s)	*MMT* (s)	Coordination factor, *k*	t_{op} (s)	*MCT* (s)	*CTI* (s)
Rc 2	**F4**	8.06	9.37	0.017	0.018	**1.06**	0.819	0.040	0.779
	F6	7.84	9.12	0.017	0.010	**0.59**	0.831	0.022	0.809
	F7	5.62	6.54	0.017	0.015	**0.88**	0.928	0.032	0.896
Rc 4	F16	4.51	5.25	0.017	0.059	3.47	0.353	0.102	0.251
Rc 5	F14	3.30	3.84	0.017	0.114	6.71	0.789	0.171	0.618
	F15	3.25	3.78	0.017	0.01	**0.59**	0.821	0.023	0.798

TABLE 23. Coordination between relay and downstream devices without considering protection constraints.

Upstream protection device	Downstream protection device and its fault location	Max. fault current (A)	Protection device operating time, (s)		
			Upstream	Down stream	*CTI*
R1, 900A	F1, 50A	6,686	3.432	0.018	3.414
	Rc1, 120A	6,705	3.396	1.989	1.407
	F3, 30 A	9,847	2.858	0.014	2.844
	Rc2 530A	9,373	2.91	0.819	2.091
R2, 562A	F9, 140A	6,631	2.761	0.067	2.694
	Rc3 250A	7,771	2.684	0.473	2.211
	Rc5, 200A	5,578	2.81	0.789	2.021
R3, 433A	Rc4, 375A	9,055	2.225	0.158	2.067
	F17, 50A	7,211	2.41	0.017	2.393

network's initial configuration. Three relays located are at the beginning of each feeder as main and backup protection, while at the beginning of the laterals are equipped with 5 reclosers (Rc) and 17 fuses (F).

To highlight the effectiveness of the proposed protection method on a large-sized network, two cases were simulated; Case 7 without protection constraints and Case 8 considering protection constraints. Details and one-line diagram of the initial configuration are shown in Table 20 and Fig. 12. Table 20 also shows the results of optimal NR for Case 7 and Case 8. Only key unique results obtained from this 118 bus case study are discussed in this section, noting that the other results are in agreement with the discussion presented in the previous case studies in Section V and VI.

The protection system requirements on coordination and fault current are similar as mention in 69 bus test system. TDS for the relay is 1.0, while TDS for reclosers in fast mode is using short-time extremely inverse of ANSI curve set at 1.0, whereas the slow mode setting is ranging from 1.0 to 3.0 using normal inverse ANSI. *CTI* is 0.2 seconds.

A. CASE 7: OPTIMAL NR WITH OPTIMUM DG SIZING WITHOUT PROTECTION CONSTRAINTS

The optimal solution for Case 7 is presented in Table 20. In this table, the proposed methods are also compared with other research works assuming the same DG locations. Result shows that FA performs better than the other method with 54.62% reduction of power loss compared to initial configurations.

TABLE 24. Protective devices condition in optimal configuration considering protection constraints with DGs connected.

Protective device	Load current (A)	Load current with 25% overload (A)	Fault current (A)		Protective Device Condition
			Min.	Max.	
Relay 1, 900A	453.28	566.60	11,036	12,833	Close
Relay 2, 562A	330.98	413.73	13,573	15,782	Close
Relay 3, 433A	169.69	212.11	14,680	17,069	Close
Recloser 1, 120A	64.86	81.07	5,765	6,703	Close
Recloser 2, 530A	358.12	447.66	6,918	8,044	Close
Recloser 3, 250A	35.10	43.87	6,979	8,115	Close
Recloser 4, 375A	180.36	225.45	7,791	9,059	Close
Recloser 5, 200A	148.80	186.00	4,744	5,517	Close
F1, 50A	30.55	38.19	5,745	6,680	Close
F2, 40A	13.43	16.78	1,479	1,720	Close
F3, 30A	16.72	20.90	4,587	5,334	Close
F4, 140A	90.68	113.35	8,155	9,482	Close
F5, 20A	5.35	6.68	1,264	1,469	Close
F6, 80A	34.79	43.49	7,913	9,202	Close
F7, 80A	62.85	78.56	6,136	7,135	Close
F8, 200A	41.82	52.27	4,748	5,521	Close
F9, 140A	82.19	102.74	3,885	4,518	Close
F10, 100A	56.91	71.14	2,282	2,654	Close
F11, 30A	15.76	19.70	2,242	2,607	Close
F12, 140A	60.30	75.38	5,782	6,724	Close
F13, 40A	0.00	0.00	1,637	1,903	Close
F14, 140A	72.62	90.77	3,277	3,811	Close
F15, 65A	43.45	54.32	3,227	3,753	Close
F16, 140A	86.57	108.21	4,510	5,244	Close
F17, 50A	28.56	35.70	6,204	7,214	Close

In terms of fulfilling the protection system requirement, Table 21 indicates that all fuses perform correctly in both normal and overload situation, except for fuses F3 and F13 which melt due to overload current while fuses F3, F7 and F13 will melt on 25% overload condition. All protective devices able to sense the minimum fault current to prevent the protection blinding.

Table 22 shows failures of coordination between recloser and downstream fuses in fast operation mode with *k* value less than 1.25. In this situation, the reclosers Rc 2 and Rc 5 will operate wrongly ahead of their respective fuses F4, F6, F7 and F15. TCC curves on coordination for recloser with downstream fuses, and relay with its downstream devices are plotted in Fig. 13 and 14, respectively.

Operating time for relay and its downstream devices, along with CTI between their operations are presented in Table 23. Fig. 14 further illustrates the coordination of the relay operating curves and its downstream devices. According to Table 16 and Fig. 14, CTI for recloser and fuse fulfil the protection coordination requirement.

B. CASE 8: OPTIMAL NR WITH OPTIMUM DG SIZING CONSIDERING PROTECTION CONSTRAINTS

Case 8 considers protection constraints in the NR optimization process to simulate a real DN operation. In terms of the objective function, Table 20 shows that the proposed solution

TABLE 25. Coordination between reclosers and downstream fuses in fast and slow mode operation without protection constraints.

Protection Device		Fault Current at Downstream (kA)		Fast Operation Mode			Slow Operation Mode		
Up stream	Down stream	Min.	Max	t_{op} (s)	*MMT* (s)	Coordination factor, *k*	t_{op} (s)	*MCT* (s)	*CTI* (s)
Rc 1	F2	1.46	1.72	0.017	0.038	2.24	0.29	0.061	0.229
Rc 2	F8	4.693	5.52	0.017	0.138	8.12	1.093	0.209	0.884
Rc 3	F12	5.715	6.72	0.017	0.035	2.06	0.473	0.067	0.406
Rc 4	F16	4.457	5.24	0.017	0.059	3.47	0.353	0.101	0.252
Rc 5	F14	3.239	3.81	0.017	0.114	6.71	0.755	0.165	0.59

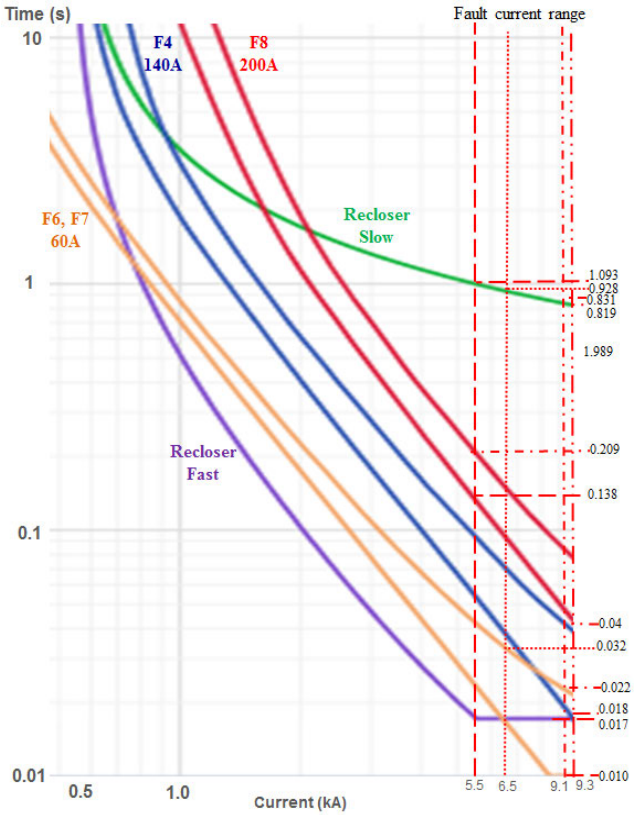

FIGURE 13. TCC coordination between recloser and downstream fuses in fast and slow mode operation generated based on Case 7 and 8 for 118-bus test system.

using FA technique performs better than EP. However, in this configuration, power loss increases compared to the optimal configuration which does not consider protection constraint. Simulation results in Table 24 show that all 25 protective devices work properly in normal loading condition as well as fault condition.

Table 25 and 26 demonstrate that coordination is held between all of the main and backup protection devices for reclosers with downstream fuses and relays with downstream devices. The coordination can be seen held in Fig.13 and 14 according to the respective fault location and fault current values.

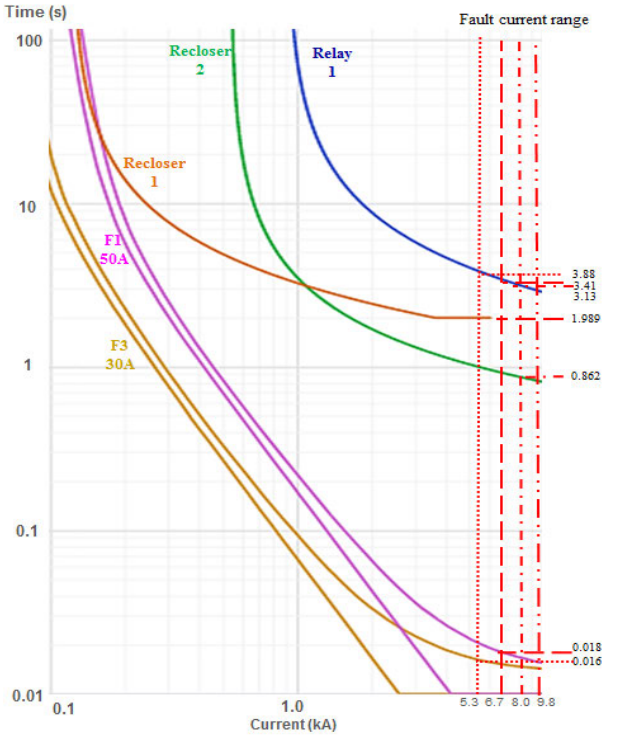

FIGURE 14. TCC coordination between relay and downstream protective devices generated based on Case 7 and 8 for 118-bus test system.

TABLE 26. Coordination between relay and downstream devices without considering protection constraints.

Upstream protection device	Downstream protection device and its fault location	Max. fault current (A)	Protection device operating time, (s)		
			Upstream	Down stream	*CTI*
R1, 900A	F1, 50A	6,679	3.411	0.018	3.393
	Rc1, 120A	6,703	3.405	1.989	1.416
	F3, 30 A	5,334	3.880	0.016	3.864
	Rc2 530A	8,044	3.135	0.862	2.273
R2, 562A	F9, 140A	4,517	3.659	0.125	3.534
	Rc3 250A	8,115	2.543	0.473	2.07
	Rc5, 200A	5,517	2.99	0.789	2.201
R3, 433A	Rc4, 375A	9,059	2.313	0.316	1.994
	F17, 50A	7,214	2.410	0.017	2.393

VIII. CONSISTENCY TEST AND COMPUTATIONAL TIME

The consistency of the proposed algorithm is evaluated based on the best, average and worst solution attained in 20 runs for each case as shown in Table 27. Total numbers of runs that produce the same optimal solutions are also presented in this table. It can be observed that for 33-bus and 69-bus system, the average power loss is very close to the optimal answer. While for a larger system of 118-bus, the differences are slightly larger within 2.49% to 4.82% due to larger search space. However, in comparison to EP, FA found to be more consistent in attaining an optimal solution.

Table 27 also presents the average processing time for each case that has been simulated on 3.10 GHz CPU, 12GB RAM

TABLE 27. Consistency test and computational time of all test systems for cases without and with consideration on protection constraints.

Test System and Cases	Proposed Tech-nique	Power loss				Avrg. time (s)	No. of runs with same optimal solutions over 20 runs
		Best (kW)	Worst (kW)	Average (kW)	Std. Dev.		
33-bus Test System							
Case 1: Without protection constraints, without DG	FA	139.50	149.50	140.20	2.30	18.74	18
	EP	139.50	165.56	141.54	6.38	17.31	18
Case 2: Considering protection constraints, without DG	FA	181.10	195.6	181.98	3.17	22.56	17
	EP	181.90	201.3	184.05	5.40	20.11	16
Case 3: Without protection constraints, with DG	FA	72.36	81.63	73.33	2.48	18.87	16
	EP	73.34	89.96	74.89	4.17	18.95	17
Case 4: Considering protection constraints, with DG	FA	91.02	103.50	92.15	3.08	29.58	16
	EP	93.30	112.45	95.11	4.51	24.1	15
69-bus Test System							
Case 5: Without protection constraints, with DG	FA	39.54	52.11	41.57	3.44	33.51	11
	EP	40.34	59.54	44.59	6.78	25.68	12
Case 6: Considering protection constraints, with DG	FA	126.8	152.30	129.57	5.90	63.72	13
	EP	150.4	171.63	153.79	7.08	51.88	12
118-bus Test System							
Case 7: Without protection constraints, with DG	FA	591.717	661.23	606.85	22.90	68.73	5
	EP	607.561	702.60	638.36	34.45	53.68	6
Case 8: Considering protection constraints, with DG	FA	659.17	720.69	683.55	19.21	254.23	5
	EP	712.29	823.36	744.90	31.13	206.33	4

desktop computer. It can be observed that in most of the cases, EP performs faster in finding the optimal solutions compared to using FA. Constraints imposed by NR and protection coordination requirements have led to more processing time for the optimization to find the best solutions. The time reported by other research works is varies depending on the CPU capability. The simulation time can be reduced by considering high power computation facilities and the associated cost incurred.

IX. CONCLUSION

Network reconfiguration with DG presence may cause unnecessary tripping and downtime to the DN, as well as equipment damages. This paper proposed an optimal NR strategy considering constraints on protection system to mitigate the impact of DG integration. The aim of the study is to find the network configuration with optimum penetration of DG, minimum power loss and smallest bus voltage deviation while ensuring protection devices remain coordinated. Protection constraints in terms of operation and coordination of the protective devices were explicitly formulated in this paper without the need to alter the existing protection schemes, inline with the practice in utility due to economical reason. A systematic approached using FA and EP was formulated to solve the optimization problem. The effectiveness of the proposed method has been verified on IEEE 33-bus, 69-bus and 118-bus.

Results from simulation prove that NR inevitably affects the protection system. NR without considering the protection constraints will result in configurations that are not practical to be implemented in actual DN. Despite lead to higher power loss as compared to the optimal configuration without protection constraint, the proposed method offers an optimal NR, as well as optimal DG sizing while protective devices are working properly. It can be concluded that FA is better than EP as an optimization tool to find the optimal result in this proposed method. In terms of consistency and computational time, it was found that 33-bus and 69-bus perform better than large test system such as 118-bus due to the size of the search space. As the penetration of DG is continuously growing, while it is costly and technically challenging to upgrade the original protection systems, the suggested method help to optimize the penetration of DGs in DN.

REFERENCES

[1] S. K. Goswami and S. K. Basu, "A new algorithm for the reconfiguration of distribution feeders for loss minimization," *IEEE Trans. Power Del.*, vol. 7, no. 3, pp. 1484–1491, Jul. 1992.

[2] S. Essallah, A. Bouallegue, and A. K. Khedher, "Optimal sizing and placement of DG units in radial distribution system," *Int. J. Renew. Energy Res.*, vol. 8, no. 1, pp. 166–177, 2018.

[3] S. R. Tuladhar, J. G. Singh, and W. Ongsakul, "Multi-objective approach for distribution network reconfiguration with optimal DG power factor using NSPSO," *IET Gener., Transmiss. Distrib.*, vol. 10, no. 12, pp. 2842–2851, Feb. 2016.

[4] B. Poornazaryan, P. Karimyan, G. B. Gharehpetian, and M. Abedi, "Optimal allocation and sizing of DG units considering voltage stability, losses and load variations," *Int. J. Elect. Power Energy Syst.*, vol. 79, pp. 42–52, Jul. 2016.

[5] M. R. Dorostkar-Ghamsari, M. Fotuhi-Firuzabad, M. Lehtonen, and A. Safdarian, "Value of distribution network reconfiguration in presence of renewable energy resources," *IEEE Trans. Power Syst*, vol. 31, no. 3, pp. 1879–1888, May 2016.

[6] R. S. Rao, K. Ravindra, K. Satish, and S. V. L. Narasimham, "Power loss minimization in distribution system using network reconfiguration in the presence of distributed generation," *IEEE Trans. Power Syst.*, vol. 28, no. 1, pp. 317–325, Feb. 2013.

[7] A. Hatata and A. Lafi, "Ant lion optimizer for optimal coordination of DOC relays in distribution systems containing DGs," *IEEE Access*, vol. 6, pp. 72241–72252, 2018.

[8] M. Norshahrani, H. Mokhlis, H. A. Bakar, J. J. Jamian, and S. Sukumar, "Progress on protection strategies to mitigate the impact of renewable distributed generation on distribution systems," *Energies*, vol. 10, no. 11, p. 1864, 2017.

[9] Y. Hsu and J.-H. Yi, "Planning of distribution feeder reconfiguration with protective device coordination," *IEEE Trans. Power Del.*, vol. 8, no. 3, pp. 1340–1347, Jul. 1993.

[10] B. Khorshid-Ghazani, H. Seyedi, B. Mohammadi-Ivatloo, K. Zare, and S. Shargh, "Reconfiguration of distribution networks considering coordination of the protective devices," *IET Gener., Transmiss. Distrib.*, vol. 11, no. 1, pp. 82–92, Jan. 2017.

[11] H. Zhan, C. Wang, Y. Wang, X. Yang, X. Zhang, C. Wu, and Y. Chen, "Relay protection coordination integrated optimal placement and sizing of distributed generation sources in distribution networks," *IEEE Trans. Smart Grid*, vol. 7, no. 1, pp. 55–65, Jan. 2016.

[12] S. A. M. Javadian, R. Tamizkar, and M.-R. Haghifam, "A protection and reconfiguration scheme for distribution networks with DG," in *Proc. IEEE Bucharest PowerTech*, Jun./Jul. 2009, pp. 1–8.

[13] O. Badran, H. Mokhlis, S. Mekhilef, and W. Dahalan, "Multi-objective network reconfiguration with optimal DG output using meta-heuristic search algorithms," *Arabian J. Sci. Eng.*, vol. 43, no. 6, pp. 2673–2686, 2018.

[14] O. Badran, H. Mokhlis, S. Mekhilef, W. Dahalan, and J. Jallad, "Minimum switching losses for solving distribution NR problem with distributed generation," *IET Gener., Transmiss. Distrib.*, vol. 12, no. 8, pp. 1790–1801, Apr. 2018.

[15] K. G. Ing, J. J. Jamian, H. Mokhlis, and H. A. Illias, "Optimum distribution network operation considering distributed generation mode of operations and safety margin," *IET Renew. Power Gener.*, vol. 10, no. 8, pp. 1049–1058, Sep. 2016.

[16] A. M. Imran, M. Kowsalya, and D. P. Kothari, "A novel integration technique for optimal network reconfiguration and distributed generation placement in power distribution networks," *Int. J. Elect. Power Energy Syst.*, vol. 63, pp. 461–472, Dec. 2014.

[17] A. M. Imran and M. Kowsalya, "A new power system reconfiguration scheme for power loss minimization and voltage profile enhancement using fireworks algorithm," *Int. J. Elect. Power Energy Syst.*, vol. 62, pp. 312–322, Nov. 2014.

[18] W. M. Dahalan, H. Mokhlis, R. Ahmad, A. H. A. Bakar, and I. Musirin, "Simultaneous network reconfiguration and DG sizing using evolutionary programming and genetic algorithm to minimize power losses," *Arabian J. Sci. Eng.*, vol. 39, no. 8, pp. 6327–6338, 2014.

[19] N. K. Roy and H. R. Pota, "Current status and issues of concern for the integration of distributed generation into electricity networks," *IEEE Syst. J.*, vol. 9, no. 3, pp. 933–944, Sep. 2015.

[20] D. Isle, M. Vaziri, M. Zarghami, and S. Vadhva, "Review of concepts to increase distributed generation into the distribution network," in *Proc. 6th Annu. Green Technol. Conf. (GreenTech)*, Apr. 2014, pp. 118–125.

[21] P. T. Manditereza and R. Bansal, "Renewable distributed generation: The hidden challenges—A review from the protection perspective," *Renew. Sustain. Energy Rev.*, vol. 58, pp. 1457–1465, May 2016.

[22] J. Kennedy, P. Ciufo, and A. Agalgaonkar, "A review of protection systems for distribution networks embedded with renewable generation," *Renew. Sustain. Energy Rev.*, vol. 58, pp. 1308–1317, May 2016.

[23] S. Conti, "Analysis of distribution network protection issues in presence of dispersed generation," *Electr. Power Syst. Res.*, vol. 79, pp. 49–56, Jan. 2009.

[24] T. T. Nguyen and A. V. Truong, "Distribution network reconfiguration for power loss minimization and voltage profile improvement using cuckoo search algorithm," *Int. J. Elect. Power Energy Syst.*, vol. 68, pp. 233–242, Jun. 2015.

[25] J. M. Gers and E. Holmes, *Protection of Electricity Distribution Networks*, vol. 47. Edison, NJ, USA: IET, 2005.

[26] M. Geidl, "Protection issues with DG," in *Protection Power Systems With Distributed Generation: State of the Art*. Zürich, Swizerland: EEH Power Systems Laboratory, ETH, Eidgenössische Technische Hochschule, 2005, pp. 7–14.

[27] *Measuring Relays and Protection Equipement—Part 151: Functional Requirements for Over/Under Current Protection*, IEC Standard 60255-151, 2009, p. 63.

[28] W. Yan, S. Lu, and D. C. Yu, "A novel optimal reactive power dispatch method based on an improved hybrid evolutionary programming technique," *IEEE Trans. Power Syst.*, vol. 19, no. 2, pp. 913–918, May 2004.

[29] M. S. Tsai and F. Y. Hsu, "Application of grey correlation analysis in evolutionary programming for distribution system feeder reconfiguration," *IEEE Trans. Power Syst.*, vol. 25, no. 2, pp. 1126–1133, May 2010.

[30] R.-H. Liang, J.-C. Wang, Y.-T. Chen, and W.-T. Tseng, "An enhanced firefly algorithm to multi-objective optimal active/reactive power dispatch with uncertainties consideration," *Int. J. Elect. Power Energy Syst.*, vol. 64, pp. 1088–1097, Jan. 2015.

[31] X.-S. Yang, "Firefly algorithms for multimodal optimization," in *Proc. Int. Symp. Stochastic Algorithms*, 2009, pp. 169–178.

[32] M. E. Baran and F. F. Wu, "Network reconfiguration in distribution systems for loss reduction and load balancing," *IEEE Trans. Power Del.*, vol. 4, no. 2, pp. 1401–1407, Apr. 1989.

[33] A. Zidan and E. F. Ei-Saadany, "Distribution system reconfiguration for energy loss reduction considering the variability of load and local renewable generation," *Energy*, vol. 59, pp. 698–707, Sep. 2013.

[34] S&C Electric Company. [Online]. Available: https://www.sandc.com/en/products–services/products/positrol-fuse-links/#Product%20Details

[35] B. de Metz-Noblat, F. Dumas, and C. Poulain, "Cahier technique No. 158: Calculation of short-circuit currents," Schneider Electr., Rueil-Malmaison, France, Tech. Rep. 158, 2005.

[36] C. Gerez, L. I. Silva, E. A. Belati, A. J. S. Filho, and E. C. M. Costa, "Distribution network reconfiguration using selective firefly algorithm and a load flow analysis criterion for reducing the search space," *IEEE Access*, vol. 7, pp. 67874–67888, 2019.

[37] T. T. Nguyen, T. T. Nguyen, A. V. Truong, Q. T. Nguyen, and T. A. Phung, "Multi-objective electric distribution network reconfiguration solution using runner-root algorithm," *Appl. Soft Comput.*, vol. 52, pp. 93–108, Mar. 2017.

[38] *IEEE Standard for Interconnecting Distributed Resources With Electric Power Systems*, IEEE Standard 1547-2003, 2003, pp. 1–28.

[39] J. S. Savier and D. Das, "Impact of network reconfiguration on loss allocation of radial distribution systems," *IEEE Trans. Power Del.*, vol. 22, no. 4, pp. 2473–2480, Oct. 2007.

[40] D. Zhang, Z.-C. Fu, and L.-C. Zhang, "An improved TS algorithm for loss-minimum reconfiguration in large-scale distribution systems," *Electr. Power Syst. Res.*, vol. 77, nos. 5–6, pp. 685–694, Apr. 2007.

[41] T. T. Nguyen, A. V. Truong, and T. A. Phung, "A novel method based on adaptive cuckoo search for optimal network reconfiguration and distributed generation allocation in distribution network," *Int. J. Elect. Power Energy Syst.*, vol. 78, pp. 801–815, Jun. 2016.

MOHAMAD NORSHAHRANI ABDUL RAHIM received the B.Eng. degree in electrical engineering from Universiti Teknologi MARA, in 2003, and the M.Eng. degree in electrical engineering from the University of Malaya (UM), Malaysia, in 2012.

He has 16 years of consulting experience. He is currently an Electrical Engineer with the Public Works Department, Ministry of Works, Malaysia. He is also a Practicing Professional Engineer in Malaysia. His current research interests include power system protection, distribution automation, and renewable energy.

HAZLIE MOKHLIS (M'01–SM'18) received the B.Eng. and M.Eng.Sc. degrees in electrical engineering from the University of Malaya (UM), Malaysia, in 1999 and 2002, respectively, and the Ph.D. degree from The University of Manchester, Manchester, U.K., in 2009.

He is currently a Professor with the Department of Electrical Engineering, UM, and the Head of the UM Power and Energy Systems (UMPES) Research Group. His research interests include fault location, distribution automation, power system protection, and renewable energy. He is a Chartered Engineer in U.K., and also a Professional Engineer in Malaysia.

ABDUL HALIM ABU BAKAR (M'04) received the B.Sc. degree in electrical engineering from Southampton University, U.K., in 1976, and the M.Eng. and Ph.D. degrees from University Technology Malaysia, in 1996 and 2003, respectively. He has 30 years of utility experience in Malaysia, before joining academia. He is currently a Professor with the University Malaya Power Energy Dedicated Advance Center (UMPEDAC), University of Malaya, Malaysia.

MIR TOUFIKUR RAHMAN received the bachelor's degree in electrical and electronic engineering from the University of Asia Pacific, Bangladesh, in 2012, and the M.Eng.Sc. degree from the University of Malaya (UM), Malaysia, in 2018. He is currently pursuing the Ph.D. degree in electrical engineering with RMIT University, Australia. His current research interests include optimization techniques, renewable energy, and distribution system modeling.

OLA BADRAN received the B.E. degree (Hons.) in electrical engineering from Palestine Technical University–Kadoorie (PTUK), Palestine, in 2008, the M.E. degree (Hons.) in clean energy engineering and conservation of consumption from An-Najah National University, Palestine, in 2012, and the Ph.D. degree from the University of Malaya, Malaysia. Her research interests include reconfiguration, optimization techniques, and renewable energy.

NURULAFIQAH NADZIRAH MANSOR received the B.Eng. degree from Vanderbilt University, USA, the M.Eng. degree in power system engineering from the University of Malaya, Malaysia, and the Ph.D. degree from The University of Manchester, U.K., in 2008, 2013, and 2018, respectively. From 2008 to 2014, she was a Process Engineer with Texas Instruments (M). She is currently a Senior Lecturer with the University of Malaya. Her research interests include distribution system modeling and optimization, distribution system planning and operation, integration of renewable energy, and smart grid.